ISSN 1069-3513, Izvestiya, Physics of the Solid Earth, 2006, Vol. 42, No. 6, pp. 449–459. © Pleiades Publishing, Inc., 2006.
Original Russian Text © M.Yu. Reshetnyak, 2006, published in Fizika Zemli, 2006, No. 6, pp. 3–13.

Hydrodynamic Helicity in Boussinesq-Type Models of the Geodynamo

M. Yu. Reshetnyak

Schmidt Institute of Physics of the Earth, Russian Academy of Sciences, Bol'shaya Gruzinskaya ul. 10, Moscow, 123995 Russia

Received October 17, 2005

Abstract—The generation of hydrodynamic helicity is considered in models of thermal convection of a rapidly rotating incompressible liquid (small Rossby numbers). It is shown that a system of cyclonic vortices arising in geodynamo models generates a large-scale hydrodynamic helicity. The spatial distribution of the helicity is analyzed as a function of the intensity of heat sources in models with various boundary conditions for the velocity field.

PACS numbers: 91.25.Cw

DOI: 10.1134/S1069351306060012

INTRODUCTION

The origination of a large-scale magnetic field in celestial bodies is related to magnetic convection processes. It is known that the magnetic field can be generated by both large-scale flows [Bullard and Gellman, 1954] and small-scale flows [Vainshtein, 1983]. In the latter case, along with small-scale fluctuating magnetic fields, large-scale fields arise [Vainshtein et al., 1980] (a synergic process), which is closely connected with the concept of the α-effect in the theory of mean fields [Krause and Rädler, 1980]. Averaging over one coordinate, e.g., over the longitude, and using an additional generation term with α, the 3-D dynamo problem could be reduced in many cases to the 2-D problem, while preserving the validity of the limitation imposed by the Cowling theorem, which precludes the generation of an axisymmetric magnetic field by an axisymmetric flow.

The origin of the α-effect consists in the fact that the mirror symmetry is violated in a convective rotating body and, as a result, the number of, e.g., clockwise rotating eddies in the northern hemisphere is systematically greater than the number of anticlockwise rotating ones [Krause and Rädler, 1980]. On the contrary, anticlockwise rotating eddies in the opposite hemisphere dominate over clockwise rotating ones. This violation of the mirror symmetry, resulting from the averaging of the Maxwell equations over turbulent pulsations, gives rise to a component of the average magnetic field $\mathbf{B}$ parallel to the average electric current $\mathbf{J} = \alpha\mathbf{B}$ (whereas the magnetic field is usually perpendicular to the current). It is this generally small parallel component of the magnetic field that is capable of closing the self-excitation circuit of the magnetic field in the Faraday phenomenon of electromagnetic induction.

The violation itself of the reflection invariance in the rotating turbulence is usually associated with the Coriolis force action on eddies moving in a medium with a zero gradient of density [Parker, 1979]. Let the density of the body decrease with its radius. Then, an ascending eddy broadens, producing a velocity component directed along the eddy radius. Accordingly, the Coriolis force arises due to the radial velocity and general rotation. This force makes the eddy rotate in the sense opposite to the general rotation. In a similar way, a descending eddy contracts, also giving rise to a radial velocity, and the Coriolis force makes the eddy rotate in the same sense as the general rotation. This results in a nonzero correlation,

$$\chi^H = \langle \mathbf{v} \cdot \mathrm{curl}\mathbf{v} \rangle, \quad (1)$$

i.e., the average helicity of the flow (here, $\mathbf{v}$ is the turbulent velocity and the broken brackets mean averaging). Correlation (1) determines the value of the α-effect (the Moffat formula):

$$\alpha = -\tau^H \chi^H/3, \quad (2)$$

where τ^H is the characteristic time of correlation. Note that the helicity $\mathbf{V} \cdot \mathrm{curl}\,\mathbf{V}$ is interesting in itself, without regard for the α-effect, because it is the integral of motion, like the kinetic energy [Kurganskii, 1993; Frik, 2003; Lesieur, 1997]. In mechanics, the original of χ^H is the squared angular momentum [Dolzhanskii, 2001]. It is remarkable that the pseudoscalar value χ^H can be estimated from symmetry considerations because a pseudoscalar can be constructed from the density gradient and angular rotation velocity (the so-called Krause formula, see for details [Reshetnyak and Sokolov, 2003]). This traditional interpretation of the α-effect is, however, of limited applicability. First of

all, the averaged flow $\bar{\mathbf{V}}$ often cannot be separated from the turbulent pulsations $\mathbf{v}$ in applied problems.[1] The relationship between the helicity and α-effect indicated above has such a simple form only in the case of locally homogeneous and isotropic turbulence. Finally, the medium in which the magnetic field is generated is often incompressible, so that the validity of the idea of expanding and compressing eddies is limited. It is worth noting that, after the α-effect has been established, the variability of density of the medium is, as a rule, neglected in dynamo models.

The limitations noted above are particularly characteristic of two very important cases of planetary and laboratory dynamos. In the laboratory experiment carried out by Frik [2003], liquid sodium used as a working medium can be considered as completely incompressible. The dynamo mechanism operates in the Earth's outer core, consisting mostly of liquid iron and having a density changing, according to current ideas, by 15–20% along the radius [*Geomagnetism*, 1988]. The situation with compressibility is similar in planets of the solar system. Moreover, the coefficient of volume expansion in the Earth's core is too small ($\sim 2 \times 10^{-5}$ K^{-1}) to generate heating-induced helicity in terms of Parker's model.

However, even the first 3-D models of the geodynamo in the Boussinesq approximation had regimes with nonzero large-scale helicity [Glatzmaier and Roberts, 1995]. Below, we consider possible mechanisms of the helicity generation in such systems and compare our results with known models of the solar dynamo, in which the generation mechanisms of the α-effect have been discussed for many years [Krivodubskii, 1984; Rüdiger and Kitchatinov, 1993].

EQUATIONS OF THE GEODYNAMO

Formulation of the Problem

We consider the geodynamo equations for an incompressible liquid ($\nabla \cdot \mathbf{V} = 0$) in a spherical layer ($r_i \le r \le r_0$) rotating about the z axis at an angular velocity Ω in a spherical coordinate system (r, θ, φ). We introduce the following units of measurement for the velocity $\mathbf{V}$, time t, pressure P, and magnetic field $\mathbf{B}$: κ/L, L^2/κ, $\rho\kappa^2/L^2$, and $2\Omega\rho\kappa\mu_0$, where L is the length unit, κ is the molecular heat conductivity coefficient, ρ is the density, and μ_0 is the magnetic constant; then, we have

$$E\mathrm{Pr}^{-1}\left[\frac{\partial \mathbf{V}}{\partial t} + (\mathbf{V}\cdot\nabla)\mathbf{V}\right] = \mathrm{curl}\mathbf{B}\times\mathbf{B} - \nabla P - \mathbf{1}_z\times\mathbf{V} + \mathrm{Ra}Tr\mathbf{1}_r + E\Delta\mathbf{V} \quad (3)$$

$$\frac{\partial T}{\partial t} + (\mathbf{V}\cdot\nabla)(T + T_0) = \Delta T.$$

The dimensionless numbers of Prandtl, Ekman, Rayleigh, and Roberts are written as $\mathrm{Pr} = \frac{\nu}{\kappa}$, $E = \frac{\nu}{2\Omega L^2}$, $\mathrm{Ra} = \frac{\alpha g_0 \delta T L}{2\Omega\kappa}$, and $q = \frac{\eta}{\kappa}$, where ν is the kinematic viscosity coefficient, α is the coefficient of volume expansion, g_0 is the gravity acceleration, δT is the unit perturbation of the temperature T relative to the equilibrium profile T_0, and η is the magnetic diffusion coefficient. The Rossby number is defined as $\mathrm{Ro} = E\mathrm{Pr}^{-1}$.

Problem (3) becomes fully defined by introducing boundary conditions at $r = r_i, r_0$. Zero boundary conditions are used for the temperature perturbations T, and, in conjunction with the profile T_0 specified above, this corresponds to fixed values of the total temperature $T_0 + T$: (1, 0). Note that variation in spherically symmetric boundary conditions for T (e.g., fixed temperature or heat flux at boundaries or various forms of heat source distribution in the core) affects weakly the generated magnetic field beginning from the onset of developed convection [Sarson et al., 1997; Reshetnyak and Steffen, 2005] but can dramatically change the regime of geomagnetic field reversals in the presence of inhomogeneities of the heat flux at the core–mantle boundary ranging within a few tens of percent [Glatzmaier et al., 1999]. Therefore, without loss of generality in what follows, we accept the condition of the first kind with fixed temperatures: $T_0 = \frac{r_i/r - 1}{1 - r_i}$ at $r_0 = 1$.

The impermeability condition $V_r = 0$ is accepted for the velocity field. The tangential velocity components V_θ and V_φ are subjected to the no-slip conditions $V_\theta = 0$ and $V_\varphi = 0$ at the boundaries $r = r_i$ and r_0 (the rigid core in some models can rotate about the z axis) [Glatzmaier and Roberts, 1995], which is typical of rigid boundaries; an alternative to these boundary conditions for the tangential velocity components is the vanishing of tangential stresses $\overleftrightarrow{\tau}$ at these boundaries: $\tau_{r\theta}, \tau_{r\varphi} = 0$ [Kuang and Bloxham, 1997; Tilgner and Busse, 1997]. Boundary conditions of these types are used in models of convection in stars with a free boundary [Chandrasekhar, 1981] (exact expressions for $\overleftrightarrow{\tau}$ in various coordinate systems can be found in [Landau and Lifshitz, 1975]). Such a type of boundary conditions, somewhat strange for the Earth's core, is related to the following. It is known that, in the first case, the generated magnetic field concentrates near rigid boundaries

[1] Many geo- and astrophysical problems are characterized by continuous velocity field spectra and do not make the separation into large and small scales used in the dynamics of average fields.

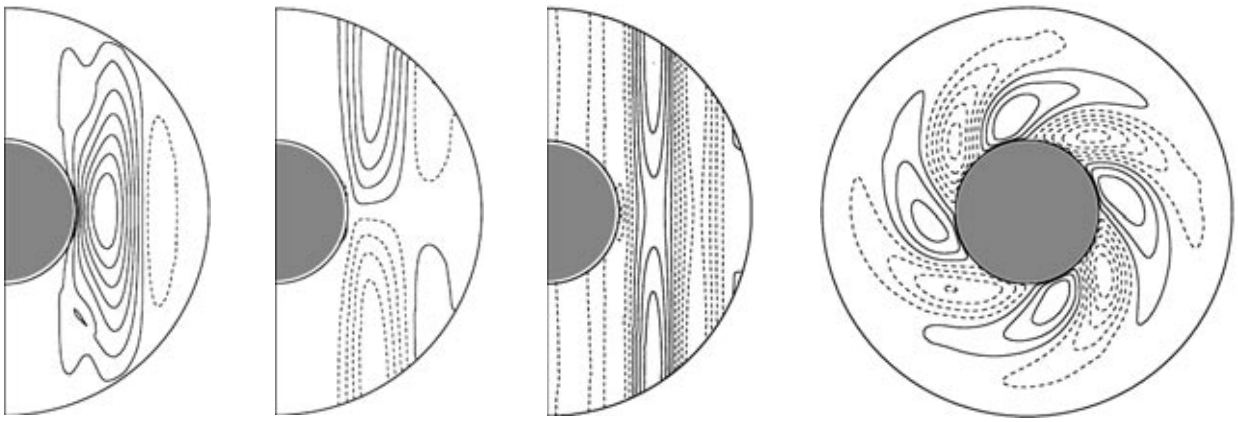

Fig. 1. Results of calculations with $E = 10^{-4}$, Pr = 1, and Ra = 10^2. The panels from left to right: the meridional cross sections of the nonaxisymmetric velocity components V_r (–4.0, 16.9), V_θ (–28.2, 28.4), and V_φ (–33.6, 38.6) and the equatorial cross section of the nonaxisymmetric velocity component V_r (–23.9, 17.3). The numbers in parentheses bound the ranges of values of the components.

(see the comparison with a nonviscous model in [Kuang and Bloxham, 1997]) and can be largely controlled by processes in Ekman layers, in which intense shear flows exist and a nonzero helicity flux is present at the rigid boundary. Given realistic values of the Ekman number $E \sim 10^{-15}$, the thickness profile the Ekman layer is $\delta_E = E^{1/2}L \sim 10^{-1}$ m, i.e., too small to account for the existing large-scale (dipole) magnetic field of the Earth. The use of the turbulent value of the viscosity coefficient does not basically change the situation: in this case, $E^T \sim 10^{-9}$ and the layer density is $\delta_E^T \sim 100$ m, which is still at the resolution threshold of modern computers. Another possibility is the use of nonviscous conditions. In this case, the magnetic field is generated in the main volume of the liquid core. In both cases, the magnetic field generated in the models has features at the Earth's surface similar to those observed by archaeo- and paleomagnetologists [*Geomagnetism*, 1988]. Below, we apply in our calculations the second type of boundary conditions in order to remove boundary effects. Vacuum boundary conditions at the outer boundary r_0 are used for the magnetic field (their numerical finite-difference implementation is described in [Hejda and Reshetnyak, 2000]).

To solve system (3) numerically, the method of control volume [Patankar, 1980; Hejda and Reshetnyak, 2003, 2004] was used and equations were solved in original physical variables on a $100 \times 100 \times 120$ grid. PC clusters and IBM SP 690+ supercomputers were used to solve the problem (methods of using parallel processors are described in detail in [Reshetnyak and Steffen, 2005]).

Modeling Results

We consider the behavior of system (3) in the absence of a magnetic field ($\mathbf{B} = 0$). An increase in the Rayleigh number Ra leads to convective instability in the form of vertical rolls [Roberts, 1965; Busse, 1970; Boubnov and Golitsyn, 1995] in distinction to hexahedra observed in an incompressible liquid (see the review in [Getling, 1999]). The rolls are known to decrease in diameter (by the law $\sim E^{1/3}$) with increasing rotation velocity of a sphere Ω. The realistic values of the Ekman number in the Earth being $E \sim 10^{-15}$, the azimuthal wave number m^{cr} at the convection generation threshold ($\mathrm{Ra} = \mathrm{Ra}^{cr}$) is estimated at $\sim 10^5$ [Jones, 2000], which is beyond the possibilities of modern numerical analysis and requires special models of turbulence [Reshetnyak and Steffen, 2004]. The situation becomes even more complicated if real values of the Rayleigh number ($\mathrm{Ra} \sim 500\ \mathrm{Ra}^{cr}$ [Jones, 2000])[2] are used.

Figure 1 presents characteristic cross sections of velocity components demonstrating the formation of vertical rolls at Ra = 100 and $\mathrm{Ra}^{cr} \sim 13$. A further increase in the Rayleigh number not only decreases the scale (Fig. 2) but also gives rise to a large-scale velocity component with wave numbers $n < m^{cr}$ well seen in the field spectra (Fig. 3). Note that the widely accepted idea of an (albeit weak) attenuation of the poloidal magnetic field at the surface of the liquid core $\sim e^{-0.1n}$ [Lowes, 1974] by no means implies (a) an attenuation of the spectrum of the entire magnetic field (including the toroidal component) throughout the liquid core volume or (b) an attenuation of the spectrum of kinetic energy (in the Earth, we have $\eta/\nu = 10^6$ and the kinetic energy spectrum is much more extended than the magnetic energy spectrum). In the absence of superviscosity effects,[3] a maximum in the kinetic energy spectrum is

[2] The Rayleigh number in the liquid core was estimated from the balance of the buoyancy and Coriolis forces.

[3] In the model of Glatzmaier and Roberts [1995], the coefficient of turbulent viscosity depends on the spectral number n as $\nu_T = \nu(1 + 0.075n^3)$.

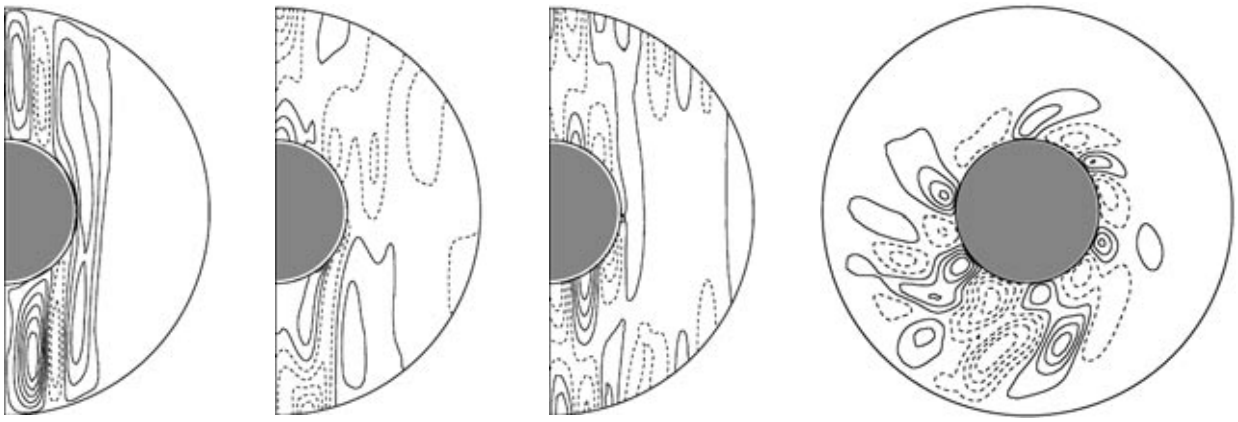

Fig. 2. Results of calculations with $E = 10^{-4}$, Pr = 1, and Ra = 5×10^2. The panels from left to right: the meridional cross sections of the velocity components V_r (–46.5, 104.6), V_θ (–111.1, 72.1), and V_φ (–132.4, 136.8) and the equatorial cross section of the nonaxisymmetric velocity component V_r (–129.6, 128.0). The numbers in parentheses bound the ranges of values of the components.

well observed in several dynamo models both with small Ra ~ 10 Ra^{cr} [Kutzner and Cristensen, 2002; Simitev, 2004] and with developed convection with Ra ≫ Ra^{cr} [Roberts and Glatzmaier, 2000].

The broadening of the region of convection wave numbers is related to both linear effects (the number of modes increases at Ra > Ra^{cr}) and the backward energy transfer along the spectrum. The latter phenomenon is well consistent with the results of linear analysis (without nonlinear terms), according to which the Rayleigh numbers should be much greater than the generally accepted estimates Ra ~ 500 Ra^{cr} in order to excite convection in the liquid core comparable in scale to the core itself [Reshetnyak, 2005b].

A characteristic feature of the two regimes considered above is the separation of the liquid core into two regions (for details and literature, see [Jones, 2000]): region I above (under) the rigid core bounded by the Taylor cylinder (TC) (the TC walls correspond to Stuartson layers) and region II outside the TC (Fig. 1). Given the excitation threshold Ra = Ra^{cr} and moderate Rayleigh numbers (Fig. 1), convection develops in region II and is virtually absent in region I, but a rise in the amplitude of heat sources (Fig. 2) shifts the convection intensity maximum into region II. However, these regions are well resolved in both cases.

As noted above, helicity (1) is generated in models with an incompressible liquid (e.g., see [Glatzmaier and Roberts, 1995], and references to many publications can be found in [Simitev, 2004]). Distributions of the hydrodynamic helicity χ^H averaged over time and the azimuthal coordinate φ are presented in Fig. 5 for the aforementioned two excitation regimes I and II. Below, we discuss the mechanisms of helicity generation and compare the inferred results with data of other studies.

HELICITY GENERATION

Helicity Models

Presently, several mechanisms of helicity generation are known. Before discussing the most widespread mechanisms, we should mention the possible generation of helicity due to reflection of Alfvén waves from rigid boundaries [Moffat, 1978; Anufriev, 1991]. This model once served as a basis for a special choice of the form of the α-effect in the geodynamo Z model [Braginsky and Roberts, 1987; Cupal and Hejda, 1992]. In terms of this model, the transition from the α-effect of the form $\alpha = \alpha_0 \cos\theta$ that is classical in the star dynamo [Zeldovich et al., 1983] to the α-effect concentrated at the core–mantle boundary was instrumental in passing from the regime of traveling waves of the solar type to a stable dipole magnetic field such that, in the main volume of the liquid core, the field is directed along the rotation axis **z**, which gave the name to the Braginsky model.

Note also the possible generation of the α-effect by shear flows, for example, in surface Ekman layer of the atmosphere [Chkhetiani, 2001]. However, it is evident that the description of helicity and the α-effect in terms of other, volume models is preferable for the modeling of large-scale magnetic fields.

On the whole, the ideas of developing volume models of helicity are based on the construction of a pseudoscalar value obtained from the scalar product of the ordinary (**G**) and axial (**w**) vectors. The Parker model [Parker, 1979], described above and the most popular in astrophysics, relates **G** to a large-scale gradient of density and uses the vorticity **w** = curl**v** as the second vector. However, this model cannot describe all possible situations. Thus, in the presence of strong magnetic fields, one should take into account the back effect of a large-scale magnetic field, tending to suppress arising small-scale flows. Then, in contrast to the hydrody-

namic (in the given case, gyrotropic) helicity, there arises the magnetic helicity χ^M, which decreases the total helicity $\chi^\Sigma = \chi^H + \chi^M$, so that $|\chi^\Sigma| \ll |\chi^H| + |\chi^M|$. The related suppression mechanism is described in [Vainshtein and Vainshtein, 1973; Krause and Rädler, 1980; Zeldovich et al., 1983], and the evolutionary equation for χ^M is presented in [Kleeorin et al., 2000]. Estimates of the helicity suppression in the Earth's liquid core are given in [Reshetnyak and Sokolov, 2003].

Although the Parker model was initially developed specially for the solar dynamo [Parker, 1979], subsequent observations of helioseismology (see the history of the problem in [Rüdiger and Kitchatinov, 1997]) provided additional constraints on the distribution of the helicity χ^H in the convective zone of the Sun: the helicity should change its sign along the radius ($\chi^H < 0$ for large r and $\chi^H > 0$ in the lower part of the convective zone), which is obviously at variance with an ascending and expanding eddy; this required a modification of numerical models [Yoshimura, 1975]. Moreover, the hypothesis on a compressible liquid in the lower part of the convective zone is inconsistent with modern ideas of the structure of the Sun.

Another scenario of the generation of helicity and the α effect proposed in [Krivodubskii, 1984; Rüdiger and Kitchatinov, 1993] was successfully applied in studies of the solar dynamo. According to this model, the α effect is determined by the kinetic energy gradient ∇E_K rather than the density gradient. Formally, this is a consequence of the fact that a pseudoscalar can be constructed from ∇E_K and the angular velocity vector $\vec{\Omega}$. This mechanism is interesting if only because spatial inhomogeneity of the kinetic energy (in both experiments and astrophysical bodies) is observed much more often than spatial inhomogeneity of density. It is worth noting that, in the case of an extremely fast rotation ($\Omega \to \infty$), the existence of $\alpha \neq 0$ can be substantiated notwithstanding the tendency of turbulence toward a 2-D pattern [Rüdiger, 1978].

These ideas of the generation of large-scale magnetic fields by small-scale turbulence in an incompressible liquid do not contradict the well-known theoretical geodynamo results [Glatzmaier and Roberts, 1995]. Below, we demonstrate the formation of the α-effect in a rotating body with variable kinetic energy using, as an example, numerical models in the Boussinesq approximation.

Sources of Helicity in an Incompressible Liquid

Before analyzing more complex helicity models, we consider possible mechanisms of the χ^H generation by the Coriolis force at a qualitative level [Vainshtein et al., 1980]. In a linear regime (small $|\mathbf{V}|$), at $\mathbf{1}_\Omega = \mathbf{1}_z$, the relation $\frac{\partial \mathbf{V}}{\partial t} \sim -\mathrm{Ro}^{-1}\mathbf{1}_z \times \mathbf{V}$ yields

$$\frac{\partial}{\partial t}(\mathbf{V} \cdot \mathrm{curl}\mathbf{V}) \sim \mathrm{Ro}^{-1}\left(\frac{\partial E_k}{\partial z} - V_z \mathrm{div}\mathbf{V} + [\mathrm{curl}\mathbf{V} \times \mathbf{V}]_z\right). \quad (4)$$

Historically, only the second term was initially taken into account, which is characteristic of gaseous bodies with high density gradients and a homogeneous distribution of kinetic energy. The continuity condition $\mathrm{div}(\mathbf{V}\rho) = 0$ yields $\mathrm{div}\mathbf{V} = -\mathbf{V} \cdot \mathbf{G}$, where $\mathbf{G} = \nabla \log \rho$, and the helicity contribution of the second term amounts to $-\mathrm{Ro}^{-1}$ $(\mathbf{G} \cdot \mathbf{1}_z)$. Evidently, with increasing rotation velocity, $\mathrm{Ro} \to 0$ and the helicity increases. This mechanism describes well the generation of the α-effect in galaxies, where $|\mathbf{G}| > 1$ [Zeldovich et al., 1983].

However, even in models of the solar dynamo [Krivodubskii, 1984; Rüdiger and Kitchatinov, 1993], the change in the helicity sign in the lower part of the convective zone could not be accounted for without invoking the helicity generation due to the spatial inhomogeneity of velocity field pulsations. In the general case, the expressions for the α-effect in the Sun have the form $\alpha \sim \nabla \ln(v_\perp \rho)$, where $v_\perp$ is the velocity pulsation component perpendicular to the rotation axis.[4]

It is evident that the contribution of the first term can be fairly large in the planetary dynamo, where the magnetic field is generated in a weakly compressible medium. Thus, the contribution of the first term in (4) to the helicity generation can already be comparable with that of the second term in the Earth's core, whose composition is accounted for by 95% molten iron and whose density varies on the core scale by $|\mathbf{G}| \sim 0.2$ [Braginsky and Roberts, 1995].

As regards the third term in (4), a more detailed analysis of flow patterns shows that the product $v_z \mathrm{curl}_z \mathbf{v}$ gives the largest contribution to the helicity and, accordingly, the third term can be neglected.

Regimes of Small Ra

Convection at the excitation threshold and comparatively small Rayleigh numbers ($\mathrm{Ra} \sim 10\ \mathrm{Ra}^{\mathrm{cr}}$) was studied in detail by Busse (see the review in [Simitev, 2004]). The convection concentrates in vertical rolls in region II and is weak in region I. In this case, the so-called weak dynamo is realized, when time-averaged magnetic and kinetic energies have the same order of magnitude.

We consider the widely used flow type independent of z (with $\mathrm{div}\mathbf{v} = 0$) [Tilgner, 1997; Jones, 2000].

[4] Since the value of turbulent pulsations in the lower convective zone of the Sun is larger compared to the overlying region and the heat exchange is convective, rather than radiative, χ^H changes its sign to the opposite.

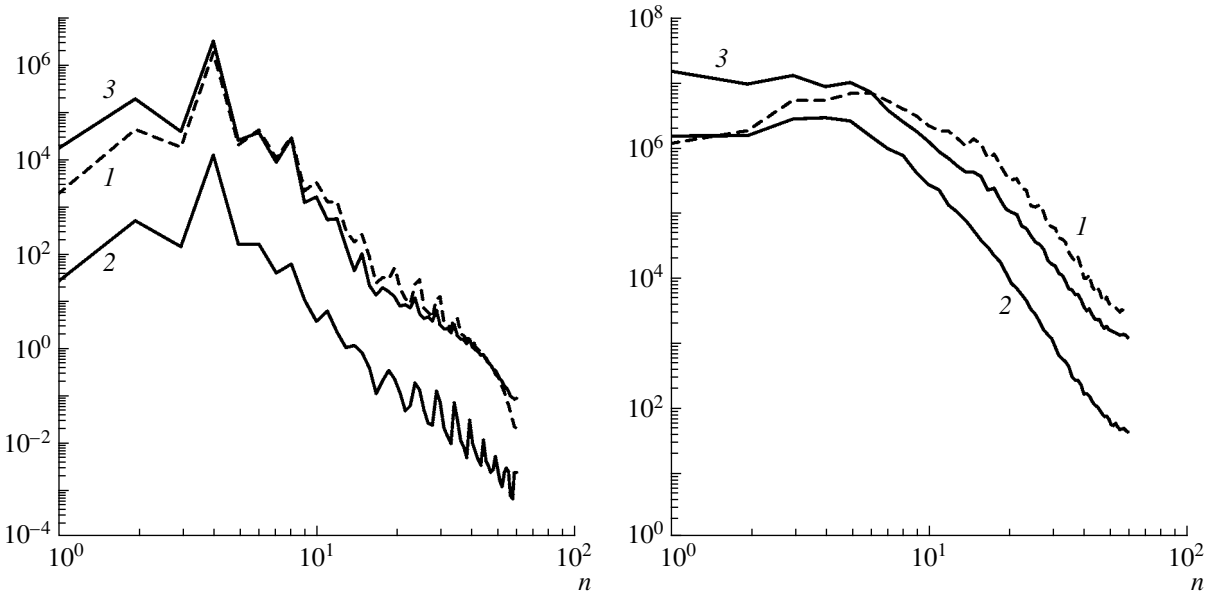

Fig. 3. Fourier spectra of the φ-components of the velocity in the azimuthal direction for two regimes (Fig. 1): (*1*) V_r; (*2*) V_θ; (*3*) V_φ.

Below, we note the stage at which the z dependence of flows becomes necessary. A roll-like flow arising in the northern hemisphere can be written by the formula

$$\mathbf{v} = (v_x, v_y, v_z) = (\sqrt{2}\sin(\pi x)\cos(\pi y), -\sqrt{2}\cos(\pi x)\sin(\pi y), -2\sin(\pi x)\sin(\pi y)). \quad (5)$$

The helicity of such a flow is always negative:

$$\chi^H = -2\sqrt{2}\pi\sin^2(\pi x)\cos^2(\pi y) - 2\sqrt{2}\pi\cos^2(\pi x)\sin^2(\pi y) - 4\sqrt{2}\pi\sin^2(\pi x)\sin^2(\pi y). \quad (6)$$

According to properties of the equatorial symmetry of flows (Fig. 1), we have in the southern hemisphere ($z < 0$) $\mathrm{curl}\,\mathbf{v}(-z) = \mathrm{curl}\mathbf{v}(z)$ and $v_z(-z) = -v_z(z)$ (for details, see [Busse, 1970]). This leads to a sign change at the equator: $\chi^H(-z) = -\chi^H(z)$. This flow is geostrophic. However, the balance alone between the pressure and the Coriolis force is insufficient for actual realization of the Busse rolls; the latter requires additionally the incorporation of the next terms in the expansion in powers of the Ekman number [Busse, 1970], accounting for the buoyancy forces and the z dependence of fields. One of the conditions following from the asymptotic analysis of such flows is the existence of finite gradients along the z axis, $|k_x| \sim |k_y| \gg |k_z| \neq 0$, where k_i is a wave number (e.g., see [Reshetnyak, 2005b]), i.e., a departure from geostrophy. With reference to a problem in a sphere, this means the influence of boundary conditions on the velocity field (Fig. 1). This statement can easily be understood, considering one of the three relations used in the linear analysis of equations, namely, the relation corresponding to the z component of the curl of the Navier–Stokes equations: $\mathrm{Ro}\,\mathrm{curl}_z\dot{\mathbf{v}} = \frac{\partial}{\partial z}v_z + E\Delta\mathrm{curl}_z\mathbf{v}$. The system is split at $k_z = 0$, and the z component of the vorticity attenuates (the condition of collinearity of the vectors $\mathbf{1_z}$ and $\mathbf{1_\Omega}$ is inessential). The presence of finite gradients in z on the main scale L is necessary for the origination of rolls. The departure from geostrophism leads to nonvanishing gradients of kinetic energy, which corresponds to the first term in (4). The latter is a necessary (but not sufficient) condition for the generation of χ^H. The generation of large-scale helicity is critically dependent on the relationship between the phases of v_z and w_z, as is evident even from the fact that, making the replacement $v_z = -v_z$ in (5), we obtain $\chi \to -\chi$. Given a layer infinite in z in the k-space, we have at the excitation threshold for the neutral mode [Reshetnyak, 2005b]: $h^c = v_z^* w_z = \frac{ik_z}{E(\mathrm{Pr}^{-1}\sigma + k^2)}|v_z|^2$. Then, we obtain $\chi = \Re h^c = \frac{2\mathrm{Pr}\omega k_z}{E(\omega^2 + |k|^4\mathrm{Pr}^2)}$, where $\omega = -i\frac{\partial}{\partial t}v/v$ is the imaginary part of the growth rate. Since the analysis of variance implies that two solutions with $\pm k$ exist for a certain value of ω (waves traveling in opposite directions), both positive ($k_z > 0$) and negative ($k_z < 0$) helicity can be generated. The total helicity vanishes, as is the case with the Alfvén waves in an infinite layer [Moffat, 1978].

The generation of nonzero helicity χ^H can be related to two effects [Busse, 1975, 1976]. These are the Ekman layers and the inclination of the layer boundary, changing the height of rolls. In the first case, a nonzero

normal component of the velocity $\sim E^{1/2}$ arises at the boundary of the Ekman layer, generating helicity ($\sim E^{1/2}$). In the northern hemisphere, the helicity is positive at the outer boundary of the core and negative at the inner core boundary. The spatial scale of the helicity in the direction normal to the boundary is comparable to the thickness of the Ekman layer $\delta_E \sim E^{1/2}$. This case is of no interest for the geodynamo theory.

The second case is more interesting. It was shown that, using the decomposition in the height of rolls depending on the distance from the rotation axis, an increase or decrease in the roll height changes the helicity sign. The effect is associated with Rossby waves shifting the rolls in the radial direction, and this movement gives rise to their additional twisting (for more details, see [Busse, 2002]). This effect was usually considered in the outer part (II) of the core, where the roll height increases with decreasing distance from the s axis. We think that precisely this phenomenon is responsible for the generation of the helicity χ inferred in [Kageyama and Sato, 1997] and from our calculations at small Rayleigh numbers (Fig. 4). The effect of boundaries leads to a negative correlation between v_z and w_z. Unlike atmospheric cyclones and anticyclones characterized by a positive correlation, the effect of boundaries yields an opposite helicity sign for region II. It is also worth noting that a decrease in the Prandtl number $\mathrm{Pr} \to 0$, shifting rolls into the equatorial zone (large s) [Zhang, 1993], can lead to a similar shift of χ^H into the equator area. However, this effect is of no significance for the Earth's core because, in models of both thermal convection ($\mathrm{Pr} \sim 0.1$) and concentration convection ($\mathrm{Pr} \sim 10$), the resulting displacement is small, particularly, at large Reynolds numbers Re ($\mathrm{Re} = \frac{VL}{\nu} \sim 10^9$ in the Earth). The values of the turbulent Prandtl number Pr^T are $\sim O(1)$ in both cases.

Moffat Estimates

Before analyzing the regime of vigorous convection, we consider some interesting consequences of the Moffat estimates with reference to the small-Ra convection model discussed above. Throughout this section, we assume that the distribution of the Busse rolls is homogeneous in the plane (x, y), perpendicular to the rotation axis z, and the fields do not vary along this axis.[5]

We decompose the velocity field into the longitudinal component along the z axis and a transverse component in the plane (x, y):

$$\mathbf{V} = \mathbf{V}_\parallel + \mathbf{V}_\perp, \quad \mathbf{V}_\parallel = \mathbf{1_z} V_z. \tag{7}$$

[5] The statistical homogeneity of a flow in the plane (x, y) corresponds to rather large values of Ra, so that rolls fill a spatial region much greater in size than their diameter.

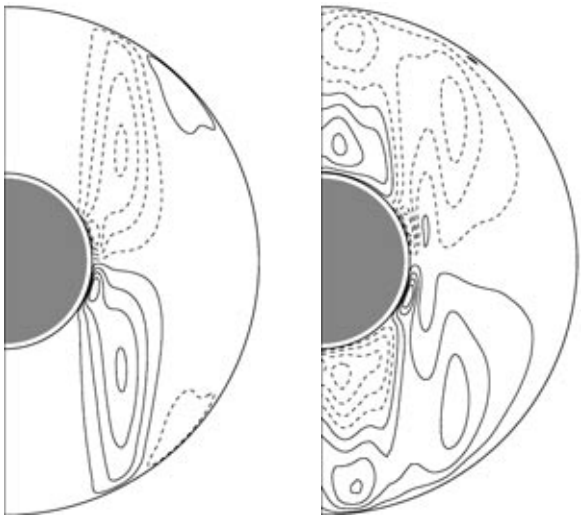

Fig. 4. Meridional cross section of the axisymmetric component of the helicity χ^H for the Rayleigh numbers $\mathrm{Ra} = 10^2$ (-6.9×10^5, 6.9×10^5) in the left panel and $\mathrm{Ra} = 5 \times 10^2$ (-3.1×10^7, 3.0×10^7) in the right panel.

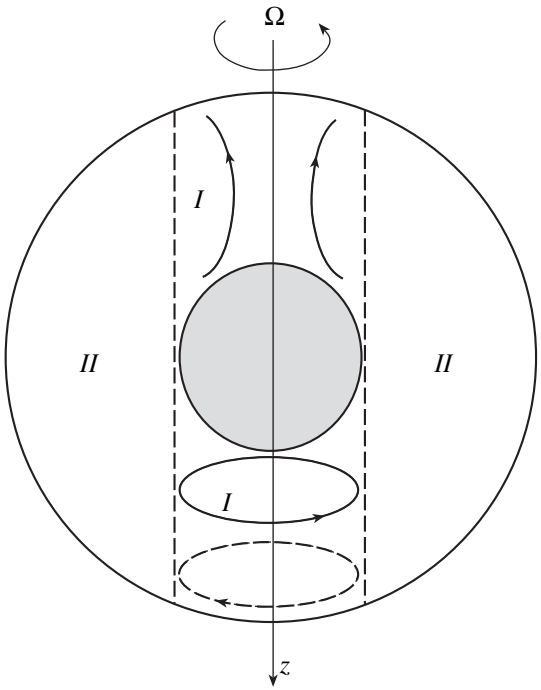

Fig. 5. The sense of the meridional circulation is shown in the upper part of the figure and the angular velocity of the liquid rotation V_φ/s is shown in the lower part.

Then, due to the homogeneity of the roll distribution in the plane (x, y), the expression for the mean helicity takes the form [Moffat, 1978]

$$\mathcal{H}^H = \langle \mathbf{V} \cdot \mathrm{curl}\mathbf{V} \rangle = \langle \mathbf{V}_\perp \cdot \mathrm{curl}\mathbf{V}_\perp \rangle + 2\langle \mathbf{V}_\parallel \cdot \mathrm{curl}\mathbf{V}_\perp \rangle. \tag{8}$$

The second term ($V_z w_z \equiv \mathbf{V}_\parallel \mathrm{curl}\mathbf{V}_\perp$) is already considered above. The first term in (8) can be estimated from the balance of the buoyancy Coriolis forces in (3):

$$\mathbf{1_z}\times\mathbf{V} = -\nabla p + \mathrm{Ra}T\mathbf{1_z}. \quad (9)$$

After applying the curl operation to (9), multiplying the result by $\mathbf{1_z}\times\mathbf{V}$, and taking into consideration (7) (for details, see [Moffat, 1978]), we obtain an estimate for the first term in (8):

$$\langle \mathbf{V}_\perp \cdot \mathrm{curl}\mathbf{V}_\perp \rangle = -\mathrm{Ra}\left\langle T\frac{\partial V_z}{\partial z}\right\rangle. \quad (10)$$

As before, we see that the dependence on z is necessary for the helicity generation. Note also that the limiting transition from the periodic flow considered above to a random flow and Moffat estimates (10) can be made only accurate to coefficients of the order of unity (Zeldovich [1984] describes in more detail a similar case of estimating the coefficients of turbulent diffusion for random and periodic flows).

Regimes of Large Ra

At large Ra, the roll mechanism of heat transfer in region II becomes insufficient and convection moves into region I, where flows driven by the buoyancy forces are parallel to the rotation axis and the Coriolis force hinders to a lesser extent the motion and the heat transport from the hotter rigid core to the outer boundary. Overall, the mean temperature in region I is higher ($T > 0$) than in region II; however, along with the mean ascending flow, the roll structure is also present in this region. Accurate estimates of the axisymmetric and asymmetric components can be found in [Glatzmaier and Roberts, 1995], but their ratio can depend strongly on the superviscosity model in use [Zhang and Jones, 1997].

Modeling at large Ra ~ 10^3 $\mathrm{Ra}^{\mathrm{cr}}$ being complicated by the development of numerical instabilities, earlier studies of the 3-D dynamo included artificial suppression of high frequencies with the use of a superviscosity [Glatzmaier and Roberts, 1995; Kuang and Bloxham, 1997]. In the case of a vanishing relative velocity at the boundary of the liquid core, a change in the helicity sign in region I is observed with increasing r: in the northern hemisphere, the helicity sign is positive in the lower part and negative in the upper part. This is the basic distinction from the small-Ra case considered above, in which the helicity χ^H does not change its sign throughout the hemisphere. Maximums of $|\chi^H|$ are close to rigid boundaries. It is also known that, in the model of Glatzmaier and Roberts [1995], the axisymmetric component accounts for 80% of the total velocity field and the angular velocity changes its sign in the TC: $V_\varphi(z)/s > 0$ ($s = r\sin\theta$) in the lower part and <0 in the upper part (Fig. 5).

Now, we compare results of these calculations with the vertical variation in the kinetic energy. In a plane layer ($\mathbf{1_z} \equiv \mathbf{1_\Omega}$), the application of the curl operation to (9) and the scalar multiplication by $\mathbf{V}$ yield

$$\frac{\partial}{\partial z}E_k = \mathrm{Ra}\nabla T \cdot (\mathbf{1_z}\cdot\mathbf{V}). \quad (11)$$

Assuming the axial symmetry and writing out the right-hand side of (11) in the spherical system of coordinates (s, φ, z), we obtain $(\nabla_s T, 0, \nabla_z T)\cdot(-V_\varphi, V_s, 0) = -V_\varphi\nabla_s T$, where $\nabla_s T$ is the so-called Archimedes wind. Estimate (11) does not contradict the numerical results reported in [Glatzmaier and Roberts, 1995] because the temperature in region I rises toward the axis, $\nabla_s T < 0$, and the Coriolis force hinders to a lesser extent the motion and the heat transfer from the hotter rigid core toward the outer core boundary and the sign change in $\frac{\partial}{\partial z}E_k$ is determined by the inversion of the azimuthal velocity $V_\varphi(z)$ (see Fig. 5; in the case of a fast rotation, the azimuthal velocity component usually has a maximum energy). As noted above, a kinetic energy varying along the z coordinate is necessary for the generation of helicity. The following scenario is possible: if region I is hotter than region II, the average of the component of V_z is positive (in the northern hemisphere). This corresponds to the flow of the liquid into the lower part of the TC (and away from its upper part) through the Ekman layer and the TC walls. The latter implies the introduction of a positive (negative) torque and, as a result, a positive (negative) torsion in the lower (upper) part of the TC, as is observed in Fig. 5. However, two problems arise in this case. These are the questions of why a positive helicity is not observed near the equator at small Ra and why, for the Ekman numbers considered here, the helicity has a scale much smaller than the observed scale.

To narrow the range of possible situations, we address thermal convection with large Rayleigh numbers (Ra = 500) and nonviscous boundary conditions. As noted above, an increase in Ra shifts convection into the TC (Figs. 1, 2). Although the use of nonviscous boundary conditions resulted in a sign-constant angular velocity of the TC liquid, which was observed in [Glatzmaier and Roberts, 1995] but was not observed in [Kuang and Bloxham, 1997], the helicity distribution remained qualitatively the same (Fig. 4): the TC value of χ^H changes its sign in the vertical direction. The numerical experiments discussed above demonstrate that the elimination of the axisymmetric component of the velocity V changes insignificantly (by ~15%) the φ-averaged helicity χ^H. The termwise analysis of the expression for χ^H

$$\chi^H = \frac{V_r}{r\sin\theta}\left(\frac{\partial}{\partial\theta}(V_\varphi\sin\theta) - \frac{\partial V_\theta}{\partial\varphi}\right) + \frac{V_\theta}{r}\left(\frac{1}{\sin\theta}\frac{\partial V_r}{\partial\varphi} - \frac{\partial}{\partial r}(rV_\varphi)\right) + \frac{V_\varphi}{r}\left(\frac{\partial}{\partial r}(rV_\theta) - \frac{\partial V_r}{\partial\theta}\right) \quad (12)$$

in this model shows that the first of the three terms in (12) makes the greatest contribution to the formation of two χ^H structures of opposite signs in the TC; i.e., as in the cases of small Ra considered above, we deal with a nonzero correlation of small-scale cyclonic flows resulting in a large-scale effect but with a smaller scale along the z axis: χ^H changes its sign. As seen from Fig. 2, eddies in the lower and upper regions of the northern hemisphere rotate in opposite senses, but the direction of the vertical velocity component remains the same all along one roll.

Since the calculations were performed for nonviscous boundary conditions, we think that the positive helicity arises at the boundary of the rigid core due to the variation in the roll height associated with the boundary curvature [Busse, 1975]: with an increase in the distance from the z axis caused by the Rossby waves, the roll height increases, which corresponds to the positive sign of the helicity near the rigid core. The spatial scale of the distributions of positive and negative helicities is $\sim(r_0 - r_i)/2$ (Fig. 4).

DISCUSSION

Apparently, direct numerical modeling fails to provide regimes with $E \sim 10^{-15}$ and $\mathrm{Ra} \sim 500E^{-1/3} = 5 \times 10^7$ and one can only hope that the model results already belong to the asymptotic regime $E \longrightarrow 0$, $\mathrm{Ra}/\mathrm{Ra}^{cr} = \mathrm{const}$. However, the fact that the effect of the helicity formation described above depends only on the tilt of the boundary and is independent of E, makes the given mechanism attractive for modeling the helicity at realistic values of parameters.

The helicity generation mechanisms considered above can exist in the Earth's liquid core along with the traditional mechanism proposed by Parker [1979] (see also [Shimizu and Loper, 2000]). The concurrent operation of both mechanisms leads to an increase in the helicity near the outer boundary and they weaken each other near the rigid core; i.e., they operate in an antiphase mode. Since the helicity in both mechanisms is antisymmetric with respect to the equatorial plane, the total helicity also possesses this property.

It is also worth noting that the form of the α-effect, concentrated near the core–mantle boundary in the Braginsky Z model and observed in our study in the TC, can be interpreted in terms of not only the reflection of Alfvén waves from a rigid boundary but also purely hydrodynamic processes near rigid boundaries. However, in this case, the model should be complemented by helicity of an opposite sign near the boundary of the rigid core (note that initially the Z model was devoid of a rigid core). The ideas of sources of α- and Ω-effects concentrated in different spatial regions were also applied in studies of the solar dynamo [Stix, 1971].

As regards the formal similarity between the inferred dependences and solar dynamo models, we should note that the existence of the kinetic energy gradient alone is insufficient for the realization of large-scale helicity. This condition is necessary for the formation of the roll flow structure, but the correlation of vorticity with the vertical velocity component requires additional conditions, in particular, an inclination of the volume boundaries.

Above, we did not touch on the problem of calculating the α-effect (2). Practical use of the above helicity estimates in large-scale dynamo models (such as the dynamo of mean fields [Krause and Rädler, 1980]) requires information on the spectra of the fields **V** and **B**. Using the simplest estimate for the mixing length, we have $\tau^H = l/v$, i.e., $\alpha \sim -v/3$. Assuming the spectrum of the velocity field to be a white noise, $v_n = \mathrm{const} = V_{wd}$, we obtain that the magnetic Reynolds number $r_m = v/(n\eta)$ on a scale of $1/n$ is ~1 even for a scale of $10^{-3}L$, so that the turbulence-driven generation of the magnetic field is ineffective. The latter imposes a constraint on the maximum number of rolls: $n_{max} \sim 10^3$ [Jones, 2000]. In the case of turbulence involving a cascade of rolls of different diameters, this constraint agrees with the estimate of the energy-carrying scale for the term $\mathrm{curl}(\alpha\mathbf{B})$ in the induction equation. The resulting amplitude of the α-effect ($\sim V_{wd}/3$) and the related value of the dynamo number $R_\alpha = \dfrac{\alpha L}{\eta}$ used in the αω-dynamo models are comparable to estimates derived in [Anufriev et al., 1997]. The use of models with a decreasing spectrum ($v_n \sim n^{-\gamma}$), i.e., the Kolmogorov turbulence with $\gamma = 1/3$, increases the energy-carrying scale (decreases n_{max}).

ACKNOWLEDGMENTS

I am grateful to F.H. Busse and D.D. Sokolov for help in my work. This work was supported by the Russian Foundation for Basic Research, project no. N03-05-64074, and INTAS, grant no. N03-51-5807.

REFERENCES

1. A. P. Anufriev, "An α-Effect on the Core Mantle Boundary," Geophys. Astrophys. Fluid Dynamics **57**, 135–146 (1991).
2. A. P. Anufriev, M. Yu. Reshetnyak, and D. D. Sokolov, "Estimation of the Dynamo Number in the Turbulent α-Effect for the Earth's Liquid Core," Geomagn. Aeron. **37**, 141–146 (1997).
3. J. M. Aurnou, D. Brito, and P. L. Olson, "Mechanics of Inner Core Super-Rotation," Phys. Earth Planet. Inter. **23**, 3401–3407 (1996).
4. B. M. Boubnov and G. S. Golitsyn, *Convection in Rotating Fluids* (Kluwer, London, 1995).
5. S. I. Braginsky and P. H. Roberts, "Model Z Geodynamo," Geophys. Astrophys. Fluid Dynamics **38**, 327–349 (1987).

6. S. I. Braginsky and P. H. Roberts, "Equations Governing Convection in Earth's Core and the Geodynamo," Geophys. Astrophys. Fluid Dynamics **79**, 1–97 (1995).
7. E. C. Bullard and H. Gellman, "Homogeneous Dynamos and Terrestrial Magnetism," Phil. Trans. R. Soc. London **A247**, 213–278 (1954).
8. F. H. Busse, "Thermal Instabilities in Rapidly Rotating Systems," J. Fluid Mech. **44**, 441–460 (1970).
9. F. H. Busse, "A Model of the Geodynamo," Geophys. J. R. Astron. Soc. **42**, 437–459 (1975).
10. F. H. Busse, "A Model of the Geodynamo," Phys. Earth Planet. Inter. **12** (4), 350–358 (1976).
11. F. H. Busse, "Convective Flows in Rapidly Rotating Spheres and Their Dynamo Action," Phys. Fluids **14** (4), 1301–1314 (2002).
12. S. Chandrasekhar, *Hydrodynamics and Hydromagnetic Stability* (Dover, New York, 1981).
13. O. G. Chkhetiani, "On the Helical Structure of the Ekman Boundary Layer," Izv. Akad. Nauk, Fiz. Atmosf. Okeana **37** (5), 614–620 (2001).
14. I. Cupal and P. Hejda, "Magnetic Field and α-Effect in Model Z," Geophys. Astrophys. Fluid Dynamics **67**, 87–97 (1992).
15. F. V. Dolzhanskii, "On Mechanical Originals of Fundamental Hydrodynamic Invariants," Izv. Akad. Nauk, Fiz. Atmosf. Okeana **37** (4), 446–458 (2001).
16. P. G. Frik, *Turbulence: Approaches and Models* (Inst. Komp'yuternykh Issledovanii, Izhevsk, 2003) [in Russian].
17. *Geomagnetism*, Ed. by J. A. Jacobs (Academic, New York, 1988).
18. A. V. Getling, *Rayleigh–Benard Convection: Structures and Dynamics* (Editorial URSS, Moscow, 1999) [in Russian].
19. G. A. Glatzmaier and P. H. Roberts, "A Three-Dimensional Convective Dynamo Solution with Rotating and Finitely Conducting Inner Core and Mantle," Phys. Earth Planet. Inter. **91**, 63–75 (1995).
20. G. A. Glatzmaier, R. S. Coe, L. Hongre, and P. Roberts, "The Role of the Earth's Mantle in Controlling the Frequency of Geomagnetic Reversals," Nature **401**, 885–890 (1999).
21. P. Hejda and M. Reshetnyak, "The Grid-Spectral Approach to 3-D Geodynamo Modeling," Computers & Geosciences **26**, 167–175 (2000).
22. P. Hejda and M. Reshetnyak, "Control Volume Method for the Dynamo Problem in the Sphere with the Free Rotating Inner Core," Studia Geophys. Geodet. **47**, 147–159 (2003).
23. P. Hejda and M. Reshetnyak, "Control Volume Method for the Thermal Convection Problem in a Rotating Spherical Shell: Test on the Benchmark Solution," Studia Geophys. Geodet. **48**, 741–746 (2004).
24. C. A. Jones, "Convection-Driven Geodynamo Models," Phil. Trans. R. Soc. London **A358**, 873–897 (2000).
25. A. Kageyama and T. Sato, "Velocity and Magnetic Field Structures in a Magnetohydrodynamic Dynamo," Phys. Plasmas **4** (5), 1569–1575 (1997).
26. N. Kleeorin, D. Moss, I. Rogachevskii, and D. Sokoloff, "Helicity Balance and Steady-State Strength of the Dynamo Generated Galactic Magnetic Field," Astron. Astrophys. **361**, L5–L8 (2000).
27. F. Krause and K.-H. Rädler, *Mean Field Magnetohydrodynamics and Dynamo Theory* (Akademie-Verlag, Berlin, 1980).
28. V. I. Krivodubskii, "Source Intensity of Magnetic Fields of the Solar αω-Dynamo," Astron. Zh. **61** (3), 540–548 (1984).
29. W. Kuang and J. Bloxham, "An Earth-Like Numerical Dynamo Model," Nature **389**, 371–374 (1997).
30. W. Kuang and J. Bloxham, "Numerical Modeling of Magnetohydrodynamic Convection in a Rapidly Rotating Spherical Shell: Weak and Strong Field Dynamo Action," J. Comput. Phys. **153**, 51–81 (1999).
31. M. V. Kurganskii, *Introduction to Large Scale Dynamics of the Atmosphere: Adiabatic Invariants and Their Applications* (Gidrometeoizdat, St. Petersburg, 1993) [in Russian].
32. C. Kutzner and U. R. Cristensen, "From Stable Dipolar towards Reversing Numerical Dynamos," Phys. Earth Planet. Inter. **131**, 29–45 (2002).
33. L. D. Landau and E. M. Lifshitz, *Course of Theoretical Physics*, Vol. 2: *The Classical Theory of Fields* (Nauka, Moscow, 1988; Pergamon, Oxford, 1975).
34. M. Lesieur, *Turbulence in Fluids* (Kluwer, London, 1997).
35. F. J. Lowes, "Spatial Power Spectrum of the Main Geomagnetic Field," Geophys. J. R. Astron. Soc. **36**, 717–725 (1974).
36. H. K. Moffat, *Magnetic Field Generation in Electrically Conducting Fluids* (Cambridge Univ., Cambridge, 1978).
37. E. N. Parker, *Cosmical Magnetic Fields: Their Origin and Their Activity* (Clarendon Press, Oxford, 1979; Mir, Moscow, 1982).
38. S. V. Patankar, *Numerical Heat Transfer a Fluid Flow* (Taylor & Francis, New York, 1980).
39. M. Yu. Reshetnyak, "Estimation of the Turbulent Viscosity in the Liquid Core of the Earth," Dokl. Akad. Nauk **400** (1), 105–109 (2005a).
40. M. Yu. Reshetnyak, "Dynamo Catastrophe, or Why the Geomagnetic Field is So Long-Lived," Geomagn. Aeron. **45** (4), 571–575 (2005b).
41. M. Yu. Reshetnyak and D. D. Sokolov, "Geomagnetic Field Intensity and Suppression of Helicity in the Geodynamo," Fiz. Zemli, No. 9, 82–86 (2003) [Izvestiya, Phys. Solid Earth **39**, 774–777 (2003).
42. M. Reshetnyak and B. Steffen, "The Subgrid Problem of Thermal Convection in the Earth's Liquid Core," Numerical Methods and Programming **5**, 41–45 (2004). http://www.srcc.msu.su/num-meth/english/index.html.
43. M. Reshetnyak and B. Steffen, "Dynamo Model in the Spherical Shell," Numerical Methods and Programming **6**, 27–32 (2005). http://www.srcc.msu.su/num-meth/english/index.html.
44. P. H. Roberts, "On the Thermal Instability of a Highly Rotating Fluid Sphere," Astrophys. J. **141**, 240–250 (1965).
45. P. H. Roberts and G. A. Glatzmaier, "A Test of the Frozen-Flux Approximation Using a New Geodynamo

Model," Phil. Trans. R. Soc. London **358**, 1109–1121 (2000).

46. R. Rüdiger, "On the α-Effect for Slow and Fast Rotation," Astron. Nachr. **299** (4), 217–222 (1978).
47. R. Rüdiger and L. L. Kitchatinov, "α-Effect and α-Quenching," Astron. Astrophys. **269**, 581–588 (1993).
48. R. Rüdiger and L. L. Kitchatinov, "The Slender Solar Tachocline: A Magnetic Model," Astron. Nachr. **318**, 273–279 (1997).
49. G. R. Sarson, C. A. Jones, and A. W. Longbottom, "The Influence of the Boundary Region on the Geodynamo," Phys. Earth Planet. Inter. **101**, 13–32 (1997).
50. H. Shimizu and D. E. Loper, "Small-Scale Helicity and α-Effect in the Earth's Core," Phys. Earth Planet. Inter. **121**, 139–155 (2000).
51. R. Simitev, Convection and Magnetic Field Generation in Rotating Spherical Fluid Shells, Ph. D., Bayreuth: Univ. Bayreuth, 2004, p. 193. http://www.phy.uni-bayreuth.de/theo/tp4/members/simitev.html.
52. M. Stix, "A Nonaxisymmetric α-Effect Dynamo," Astron. Astrophys. **13** 203–208 (1971).
53. A. Tilgner, "A Kinematic Dynamo with a Small Scale Velocity Field," Phys. Lett. **A226**, 75–79 (1997).
54. A. Tilgner and F. H. Busse, "Finite Amplitude in Rotating Spherical Fluid Shells," J. Fluid Mech. **332**, 359–376 (1997).
55. S. I. Vainshtein, *Magnetic Fields in Cosmos* (Nauka, Moscow, 1983) [in Russian].
56. L. L. Vainshtein and S. I. Vainshtein, "On the Possibility of a Linear Turbulent Dynamo," Geomagn. Aeron. **13** (1), 149–153 (1973).
57. S. I. Vainshtein, Ya. B. Zeldovich, and A. A. Ruzmaikin, *Turbulent Dynamo in Astrophysics* (Nauka, Moscow, 1980) [in Russian].
58. H. Yoshimura, "A Model of the Solar Cycle Driven by the Dynamo Action of the Global Convection in the Solar Convection Zone," Astrophys. J. Suppl. **29**, 467–494 (1975).
59. Ya. B. Zeldovich, *Selected Works: Chemical Physics and Fluid Dynamics* (Nauka, Moscow, 1984) [in Russian].
60. Ya. B. Zeldovich, A. A. Ruzmaikin, and D. D. Sokoloff, *Magnetic Fields in Astrophysics* (Gordon and Breach, New York, 1983).
61. K. Zhang, "On Equatorially Trapped Boundary Inertial Waves," J. Fluid Mech. **248**, 203–217 (1993).
62. K. Zhang and C. A. Jones, "The Effect of Hyperviscosity on Geodynamo Models," Geophys. Res. Lett. **24**, 2869–2872 (1997).